HHS Public Access

Author manuscript

Biochim Biophys Acta. Author manuscript; available in PMC 2018 June 01.

Published in final edited form as:

Biochim Biophys Acta. 2017 June ; 1863(6): 1640–1653. doi:10.1016/j.bbadis.2017.03.010.

Identification of a molecular signaling gene-gene regulatory network between GWAS susceptibility genes *ADTRP* and *MIA3/TANGO1* for coronary artery disease

Chunyan Luo[a,1], **Fan Wang**[b,c,1], **Xiang Ren**[a,1], **Tie Ke**[a,1], **Chengqi Xu**[a,1], **Bo Tang**[a], **Subo Qin**[a], **Yufeng Yao**[a], **Qiuyun Chen**[b,c,*], and **Qing Kenneth Wang**[a,b,c,**]

[a]The Key Laboratory of Molecular Biophysics of the Ministry of Education, College of Life Science and Technology, Center for Human Genome Research, Cardio-X Institute, Huazhong University of Science and Technology, Wuhan, 430074, Hubei Province, P. R. China

[b]Center for Cardiovascular Genetics, Department of Molecular Cardiology, Lerner Research Institute, Department of Cardiovascular Medicine, Cleveland Clinic, Cleveland, Ohio, 44195, U.S.A

[c]Department of Molecular Medicine, Department of Genetics and Genome Science, Case Western Reserve University, Cleveland, OH, 44195, USA

Abstract

Coronary artery disease (CAD) is the leading cause of death worldwide. GWAS have identified >50 genomic loci for CAD, including *ADTRP* and *MIA3/TANGO1*. However, it is important to determine whether the GWAS genes form a molecular network. In this study, we have uncovered a novel molecular network between *ADTRP* and *MIA3/TANGO1* for the pathogenesis of CAD. We showed that knockdown of *ADTRP* expression markedly down-regulated expression of *MIA3/TANGO1*. Mechanistically, *ADTRP* positively regulates expression of *PIK3R3* encoding the regulatory subunit 3 of PI3K, which leads to activation of AKT, resulting in up-regulation of *MIA3/TANGO1*. Both *ADTRP* and *MIA3/TANGO1* are involved in endothelial cell (EC) functions relevant to atherosclerosis. Knockdown of *ADTRP* expression by siRNA promoted oxidized-LDL-mediated monocyte adhesion to ECs and transendothelial migration of monocytes,

[*]Corresponding author at: Center for Cardiovascular Genetics, Department of Molecular Cardiology, Lerner Research Institute, Department of Cardiovascular Medicine, Cleveland Clinic, Cleveland, Ohio, 44195, U.S.A. chenq3@ccf.org (Q.C). [**]Corresponding author at: College of Life Science and Technology, Center for Human Genome Research, Cardio-X Institute, Huazhong University of Science and Technology, Wuhan, 430074, Hubei Province, P. R. China, qkwang@hust.edu.cn, wangq2@ccf.org (Qing Kenneth Wang).

[1]These authors contributed equally to this article.

Conflict of interest

The authors declare that they have no competing interests. Some other research on *ADTRP* in the Center for Human Genome Research have receive funding from Bayer Health.

Author Contributions

QKW, CL, and QC designed the study. CL, FW, CX, XR, TK, BT, SQ, YY, performed experiments. CL, FW, CX, XR, TK analyzed data and interpreted results of experiments. QKW and CL drafted manuscript. QKW, CL, FW and QC edited and revised manuscript. QKW and QC supervised the entire project.

inhibited EC proliferation and migration, and increased apoptosis, which was reversed by expression of constitutively active AKT1 and *MIA3/TANGO1* overexpression, while the over-expression of *ADTRP* in ECs blunted these processes. Knockdown of *MIA3/TANGO1* expression also promoted monocyte adhesion to ECs and transendothelial migration of monocytes, and *vice versa* for overexpression of *MIA3/TANGO1*. We found that *ADTRP* negatively regulates the levels of collagen VII and ApoB in HepG2 and endothelial cells, which are downstream regulatory targets of MIA3/TANGOI. In conclusion, we have uncovered a novel molecular signaling pathway for the pathogenesis of CAD, which involves a novel gene-gene regulatory network. We show that *ADTRP* positively regulates *PIK3R3* expression, which leads to activation of AKT and up-regulation of *MIA3/TANGO1*, thereby regulating endothelial cell functions directly relevant to atherosclerosis.

Keywords

Coronary artery disease (CAD); Myocardial infarction (MI); *ADTRP*; *MIA3* (TANGO1); *AKT*; PI3K; Collagen VII; ApoB

1. Introduction

Coronary artery disease (CAD) is the leading cause of death worldwide. CAD is caused by atherosclerosis in the wall of coronary arteries, a pathogenic process initiated by the binding of blood monocytes to the endothelium activated by oxidized LDL cholesterol and other inflammatory molecules [1]. The adherent monocytes then migrate across the endothelium, move into the intima area and become macrophages. After uptake of modified lipoprotein particles, the macrophages are transformed into foam cells, forming an early atherosclerotic lesion and starting plaque build-up [1]. The proliferation of vascular smooth muscle cells and migration to the lesion area, degradation of the arterial extracellular matrix (collagens), and deposit of degraded products and apoptotic cell debris make the plaque grow. The inflammatory process or another insult can lead to the disruption of the endothelial barrier, leading to plaque fissure, erosion, or frank rupture, which are accompanied by tissue factor release, platelet activation, thrombosis and myocardial infarction (MI) [1].

GWAS have identified >50 genomic variants or loci associated with CAD and MI. The first GWAS for CAD and MI in the Chinese population using the GeneID database identified an intronic single nucleotide polymorphism (SNP) rs6903956 in the *C6orf105* gene (now referred to as *ADTRP*) that increases risk of CAD and MI and is associated with decreased expression of *ADTRP* [2]. The association was replicated by other groups [3–6]. *ADTRP* encodes an Androgen-Dependent TFPI-Regulating Protein, a cell surface protein with six transmembrane domains. The ADTRP protein was found to be co-localized with CAV1 in the caveolae on the cell surface and to positively regulate the expression of TFPI in endothelial cells (ECs), resulting in inhibition of FXa involved in coagulation and thrombosis [7]. *ADTRP* was later found to be expressed in human macrophages and atherosclerotic lesions, and regulated by the transcription factor Peroxisome Proliferator-Activated Receptor (PPAR)γ [8].

GWAS also revealed another significant CAD risk variant, SNP rs17465637 in an intron of the *MIA3/TANGO1* gene encoding ARNT or TANGO1[9]. We replicated the finding in an American Gene Bank Caucasian population [10] and a Chinese GeneID population [11]. A large meta-analysis with 7263 CAD patients and 8347 controls combined from five Asian populations also identified significant association between SNP rs17465637 and CAD and MI [11]. The MIA3/TANGO1 protein was found to be involved in export of collagen VII and ApoB from the endoplasmic reticulum (ER) to the Golgi apparatus and secretion of collagens I, II, III, IV, VII, and IX [12–14], which may be associated with atherosclerosis and MI [15].

In this study, we investigated the molecular mechanism by which *ADTRP* regulates endothelial cell phenotypes related to atherosclerosis and found that *ADTRP* positively regulates expression of *MIA3/TANGO1* by activating the AKT signaling pathway. These new data identify a novel biological pathway involving a novel gene-gene regulatory network for the pathogenesis of CAD.

2. Materials and methods

2.1. Plasmids and siRNAs

An expression plasmid for *ADTRP*, pCDNA3.1(−)-ADTRP, was constructed as described previously [16]. The full-length cDNA for *AKT1* (NC_000014.9; EntrezGeneID207; Ensembl: ENSG00000142208) was obtained by RT-PCR analysis using RNA samples isolated from HUVECs. The PCR product was digested with *EcoRI* and *BamHI* (TAKAKA, Japan) and sub-cloned into the multiple cloning site of pCDNA3.1(−), resulting in an expression plasmid for *AKT1*, pCDNA3.1(−)-AKT1. The cDNA for constitutively active myristoylated human *AKT1* (*myrAKT1*, 1,443 bp, 480 aa) was then obtained by PCR analysis using pCDNA3.1(−)-AKT1 as template and primers F-*EcoRI* (5′-CCGGAATTCTGGGTAGCAACAAGAGCAAGCCCAAGGATGCCAGCCAGCGGATGAGCGACGTGGCTATTGTGAA-3′) containing the Src myristoylation sequence (underlined) and R-*BamHI* (5′-CGCGGATCCTCAGGCCGTGCCGCTGGC-3′). The PCR product was digested with *EcoRI* and *BamHI* (TaKaRa Biotechnology Co., Ltd, Dalian, Liaoning, China) and subcloned into the multiple cloning site of eukaryotic expression vector pcDNA3.1(−), resulting in pcDNA3.1(−)-hmyrAKT1.

The expression plasmids for *MIA3/TANGO1*, pcDNA3.1(+)-TANGO1-HA, were as described previously [12, 14, 17–20] and kindly provided by Dr. Vivaek Malhotra and colleagues.

Small interfering RNA (siRNA) specific for human *ADTRP* (*ADTRP* siRNA), human *MIA3/TANGO1* (*MIA3/TANGO1* siRNA) and negative control siRNA (NC siRNA) were purchased from Genepharma (Suzhou, China). The sequences of siRNAs are: *ADTRP* siRNA: 5′-GGAUCCUCUUUCUCUACAATT-3′/5′-UUGUAGAGAAAGAGGAUCCTT-3′; Negative control (NC) siRNA: 5′-UUCUCCGAACGUGUCACGUTT-3′/5′-ACGUGACACGUUCGGAGAATT-3′; *MIA3/TANGO1* siRNA: 5′-GGUGAAGUCUGAAUGCCAUTT-3′/5′-AUGGCAUUCAGACUUCACCTT-3′; *PIK3R3* siRNA: 5′-

GGACUUGCUUUAUGGGAAA dTdT-3′/5′-UUUCCCAUAAAGCAAGUCC dTdT-3′; *AKT1* siRNA: 5′-GUGGACCACUGUCAUCGAA dTdT-3′/5′-UUCGAUGACAGUGGUCCAC dTdT-3′.

2.2. Cell culture and transfection

HepG2 cells, primary human umbilical vein endothelial cells (HUVECs) and EAhy926 endothelial cells were from ATCC (American Type Culture Collection, USA), Pricells (Wuhan, Hubei, China) and Shanghai Institute of Biochemistry and Cell Biology of SIBCB (Shanghai, China), respectively. Cells were maintained, cultured, and transfected with siRNA (80 nM) and plasmid DNA (2 μg) as described [21, 22]. Transfection of siRNA and plasmid DNA into EAhy926 cells was carried out using the Fu GENE® HD Transfection Reagent (Promega, Madison, Wisconsin, USA). Transfection of siRNA and plasmid DNA into other cells was performed using Lipofectamine® RNAi MAX and Lipofectamine®2000, respectively. For transfection of endothelial cells with plasmid DNA, the efficiency was too low for HUVECs and therefore the study was performed for EAhy926 endothelial cells only.

2.3. Expression analysis

Quantitative real-time reverse-transcription PCR (qRT-PCR) analysis was performed as described by us [23, 24]. All qRT-PCR reactions were run in triplicate and each experiment was repeated at least three times. The primer sequences used for qRT-PCR are as follows:

ADTRP Forward: 5′-GCCGCATCCTATGGCTCTACTTTG-3′

ADTRP Reverse: 5′-CAAGTAGGTAGATGCTGGCGATGA-3′

MIA3/TANGO1 Forward: 5′-TACAAGCGGAGAATTGAAGAAATGG-3′

MIA3/TANGO1 Reverse: 5′-GCCAGTTTTCATGAGCTTTCTTCT-3′

GAPDH Forward: 5′-ATGGGGAAGGTGAAGGTCG-3′

GAPDH Reverse: 5′-GGGGTCATTGATGGCAACAATA-3′

PIK3R3 Forward: 5′-ATGTACAATACGGTGTGGAGTATG-3′

PIK3R3 Reverse: 5′-GCTGGAGGATCCATTTCAAT-3′

AKT1 Forward: 5′-CGGGACCTCAAGCTGGAGAACCTC-3′

AKT1 Reverse: 5′-CCAGCACCTCGGGGGCCAG-3′.

Western blot analysis was carried out as described [25, 26]. The primary antibodies used for Western blotting analysis include a rabbit polyclonal antibody against ADTRP (*C6orf105*) (1:800 dilution; Sigma, MO, USA), two rabbit polyclonal antibodies against total AKT and phosphorylated AKT (1:1000; Cell Signaling Technology, MA, USA), a rabbit polyclonal antibody against MIA3/TANGO1 (1:500; Santa Cruz Biotechnology(Dallas, Texas, USA), a rabbit polyclonal antibody against GAPDH (1:1000; Cell Signaling Technology, MA, USA), a mouse monoclonal antibody against α-tubulin (1:5000; Merck Millipore, a part of Merck KGaA, Darmstadt, Germany), a rabbit polyclonal antibody against β-actin (1:1000; Cell Signaling Technology, MA, USA), a polyclonal anti-goat antibody against ApoB (1:1000, Abcam, MA, USA), and a rabbit polyclonal antibody collagen VII antibody (1:500, Abcam,

MA, USA). The secondary antibodies were either FITC labeled rabbit anti-goat antibody and goat anti-rabbit antibody (Thermo Fisher Scientific).

Immunostaining analysis was carried out for collagen VII and ApoB as described [14]. The primary antibodies were a polyclonal anti-goat antibody against ApoB (1:300) and a rabbit polyclonal antibody collagen VII antibody (1:200, Abcam, MA, USA). The secondary antibodies were either FITC labeled rabbit anti-goat antibody and goat anti-rabbit antibody (Thermo Fisher Scientific, Waltham, MA USA). The immunostaining signals were detected using Olympus 81 FV1000.

2.4. Characterization of endothelial cell functions and phenotypes

An assay for monocyte adhesion to ECs was carried out as described [27]. In brief, EAhy926 endothelial cells were transfected with siRNA or/and plasmid DNA, seeded at a density of 8×10^4 cells/well in 6-well plates, grown to fully confluent and stimulated with oxidized LDL (0.8 mg/ml ox-LDL, Yesen, Shanghai, China) for 6 h. Human HL-60 promyelocytic leukemia cells were cultured in Roswell Park Memorial Institute 1640 media supplemented with 20% fetal bovine serum (FBS, Gibco, Life Technologies, CA, USA), fluorescently labeled with Calcein AM (Fanbo, Beijing, China) for 60 min at 37°C, and seeded into each well coated with endothelial cells. After 1 h, the media were removed and fluorescent intensity was measured in each of the 6 wells with a standard fluorometer with an inverse microscope (Nikon, The Tokyo metropolitan, Japan). The fluorescent units in each well (exit: 490 nm, emission: 515 nm) was determined and analyzed using Image Pro Plus6.0 software (Media Cybernetics, Bethesda, MD, USA) to measure the number of HL-60 cells adhered to EAhy926 endothelial cells. Each experiment was repeated at least three times.

Transmigration of monocytes across endothelial cells was analyzed as described [27]. In brief, HL-60 cells (3×10^5) were pipetted into 0.4 μm pore chambers (Corning) within a Boyden chamber, which were coated or plated with EAhy926 ECs transfected with siRNA or plasmid DNA. Twenty-four hours after the transfection, cells were then stimulated for 6 h with 0.25 μg of ox-LDL. The HL-60 cells migrated to the bottom of the chamber were counted from the bottom chamber 24 h after their administration under an Olympus 81 FV1000 microscope. Each experiment was repeated at least three times.

A cell proliferation assay was carried out using Cell Counting Kit-8 (Dojindo, Kumamoto, Japan) as described [16, 27]. Each experiment was repeated at least three times.

Cell cycle analysis was performed with flow cytometry using Beckman Coulter Cytomics FC 500 (Beckman Coulter, CA, USA) as described [16, 27]. Each experiment was repeated at least three times.

An apoptosis assay was carried out with an Annexin V-FITC apoptosis analysis kit (SUN GENE Biotech, Tianjin, China) using Beckman Coulter Cytomics FC 500 as described [16, 27]. Each experiment was repeated at least three times.

A scratch-based cell migration assay was carried out as described [16, 27]. Each experiment was repeated at least three times.

A matrigel-based endothelial tube formation assay for angiogenesis was carried out as described [16, 25–27]. Each experiment was repeated at least three times.

2.5. Statistical analysis

Each experiment was repeated at least three times. For descriptive analysis, quantitative data were presented as mean ± standard error of the mean (SEM). In the functional studies, the means between two groups and among three or more groups were compared by a two-tailed Student's *t*-test and ANOVA, respectively, as implemented in SPSS version16.0 software (SPSS, Chicago, IL, USA). Statistical significance was considered at a *P* value of <0.05.

3. Results

3.1. ADTRP positively regulates expression of MIA3/TANGO1

We performed a global gene expression analysis using microarrays with knockdown of *ADTRP* expression in HepG2 cells using siRNA [16] and found that one of the candidate downstream genes of *ADTRP* is *MIA3/TANGO1*, a CAD susceptibility gene identified by GWAS [9, 11]. Using an independent set of HepG2 cells transfected with *ADTRP* siRNA and negative control siRNA (NC siRNA), we confirmed that siRNA knockdown of *ADTRP* expression by 80% reduced the expression level of *MIA3/TANGO1* by 75% ($P<0.0001$; Fig. 1A). Similar real-time RT-PCR analysis using human umbilical vascular endothelial cells (HUVECs) also revealed that siRNA knockdown of *ADTRP* expression by 70% reduced the expression level of *MIA3/TANGO1* by 67% ($P<0.0001$; Fig. 1B).

Overexpression of *ADTRP* in HepG2 cells by transient transfection of an expression plasmid for *ADTRP* (vs. empty vector control) by 56-fold also dramatically increased the expression level of *MIA3/TANGO1* by 31-fold ($P<0.001$; Fig. 1C). Similar real-time RT-PCR analysis using endothelial cells (EAhy926) also revealed that overexpression of *ADTRP* by 32-fold increased the expression level of *MIA3/TANGO1* by 9-fold ($P<0.001$; Fig. 1D).

Western blot analysis using HepG2 cell extracts revealed that knockdown of *ADTRP* expression by siRNA significantly reduced the expression level of *MIA3/TANGO1* ($P<0.001$; Fig. 1E and 1F). Similar results were obtained using ECs ($P<0.01$; Fig. 1G and 1H).

3.2. ADTRP positively regulates expression of MIA3/TANGO1 by positive regulation of PIK3R3 and activation of AKT

Because ADTRP is a plasma membrane protein, we hypothesized that ADTRP exerted its effect on gene expression by a signal transduction pathway. Therefore, we examined the list of *ADTRP* downstream genes with a potential role in cellular signaling from a microarray gene expression analysis previously reported [16]. We identified *PIK3R3* as an interesting candidate as it encodes the regulatory subunit 3 of PI3K involved in the PI3K-AKT signaling pathway [16]. Independent real-time RT-PCR studies confirmed that *ADTRP* indeed positively regulated the expression level of *PIK3R3* in both HepG2 cells and ECs [16]. Because PIK3R3 is a key regulatory subunit of PI3K that activates AKT, we

determined whether *PIK3R3* knockdown affects phosphorylation of AKT. Compared with HepG2 cells transfected with NC-siRNA, cells transfected with *PIK3R3* siRNA showed a significantly reduced level of AKT phosphorylation ($P<0.001$; Fig. 2D, 2E). Similar results were obtained from EAhy926 ECs ($P<0.001$; Fig. 2F, 2G). On the other hand, *PIK3R3* siRNA did not affect the expression levels of total AKT protein (Fig. 2D–2G) or *AKT1* mRNA (Fig. 2A–2C) in EAhy926 cells, HUVECs or HepG2 cells.

We then determined whether *PIK3R3* regulates the expression level of *MIA3/TANGO1*. Interestingly, *PIK3R3* siRNA significantly reduced the expression level of *MIA3/TANGO1* in all three cell lines tested, including EAhy926 cells, HUVECs or HepG2 cells (Fig. 2H–2J).

Based on the above data, we hypothesized that *ADTRP* regulates the expression level of *MIA3/TANGO1* by mediating activation of AKT. In EAhy926 ECs, *ADTRP* siRNA reduced the phosphorylation level of AKT by 2.9 fold ($P<0.001$; Fig.3A and 3B), whereas overexpression of *ADTRP* increased the level of AKT activation by 2.7 fold ($P<0.001$, Fig. 3A and 3B). In HepG2 cells, *ADTRP* siRNA reduced the phosphorylation level of AKT by 2.9 fold ($P<0.001$; Fig. 3C and 3D), whereas overexpression of *ADTRP* increased the level of AKT activation by 3.2 fold ($P<0.001$, Fig. 3C and 3D).

The regulation of *MIA3/TANGO1* expression by AKT was further confirmed by experiments with knockdown of *AKT1* expression by siRNA or overexpression of a constitutively active myristoylated human AKT1 (myrAKT1). Real-time RT-PCR analysis showed that *AKT1* siRNA reduced its own expression by 3.0 and 3.3 fold ($P<0.001$, Fig. 4A and 4B) and the expression level of *MIA3/TANGO1* by 2.0 fold ($P<0.001$, Fig. 4A and 4B) in HUVECs and EAhy926cells, respectively. Overexpression of *myrAKT1* by 3.8 fold increased the expression level of *MIA3/TANGO1* by 2.0 fold in EAhy926 cells ($P<0.001$, Fig. 4C). Similar results were obtained from HepG2 cells (Fig. S1).

Western blot analysis showed that the expression level of the MIA3/TANGO1 protein was reduced by 2.0 fold when *AKT1* was knockdown ($P<0.001$, Fig. 4D and 4E), but increased by 4.0 fold with overexpression of constitutively active AKTs in EAhy926 cell ($P<0.001$, Fig. 4D and 4E). Similar results were obtained in HepG2 cells (Fig. S1).

To further show that *ADTRP* regulates *MIA3/TANGO1* expression through the AKT signaling pathway, we co-expressed *myrAKT1* together with *ADTRP* siRNA in EAhy926 cells and found that overexpression of *myrAKT1* can restore the decreased *MIA3/TANGO1* expression by *ADTRP* siRNA (Fig. 4F and 4G). Similar results were obtained with HepG2 cells (Fig. S1). Furthermore, we tested the effect of LY294002, a PI3K inhibitor that inhibits AKT activation, on upregulation of *MIA3/TANGO1* by *ADTRP*. As shown in Fig. 4H and 4I, overexpression of *ADTRP* increased MIA3/TANGO1 expression by 3.0 fold, but the effect was eliminated by LY294002. Similar results were obtained in HepG2 (Fig. S1). All these data indicate that *ADTRP* regulates expression of *MIA3/TANGO1* by the AKT signaling pathway.

3.3. ADTRP and MIA3/TANGO1 regulate endothelial cell phenotypes relevant to atherosclerosis

To identify the molecular and cellular mechanisms by which *ADTRP* regulates atherosclerosis and CAD, we investigated monocyte adhesion to the endothelium (a layer of ECs), the first event involved in the initiation of atherosclerosis, and trans-endothelial migration of monocytes, a key step in atherosclerosis [27]. EAhy926 ECs transfected with *ADTRP* siRNA and stimulated with oxidized-LDL (ox-LDL) showed adhesion of a significantly increased number of HL-60 cells compared with NC siRNA ($P<0.0001$; Fig. 5A, 5E). Overexpression of *ADTRP* in EAhy926 cells significantly decreased monocyte adhesion to EAhy926 cells after stimulation of ox-LDL ($P<0.0001$; Fig. 5A, 5F). Little monocyte adhesion to EAhy926 cells was detected in the absence of ox-LDL (Fig. 5B, 5D).

Overexpression of *myrAKT* in EAhy926 cells significantly decreased HL-60 cell adhesion to EAhy926 cells ($P<0.0001$, compare NC siRNA and NC siRNA+ AKT; Fig. 5A, 5C, 5E). Overexpression of *myrAKT* also eliminated the stimulating effect of *ADTRP* siRNA on HL-60 cell adhesion to EAhy926 cells (Fig. 5A, 5C, 5E). Overexpression of both *ADTRP* and *myrAKT* further reduced the decreased level of HL-60 cell adhesion to EAhy926 cells from the levels of either overexpression of *ADTRP* or *myrAKT* (Fig. 5A, 5C, 5F).

EAhy926 ECs transfected with *MIA3/TANGO1* siRNA and stimulated with ox-LDL showed adhesion of a significantly increased number of HL-60 cells compared with NC siRNA ($P<0.0001$; Fig. 5A, 5G). However, no effect was observed for overexpression of *ADTRP* on the stimulating function of *MIA3/TANGO1* siRNA on monocyte adhesion (Fig. 5C, 5G), consistent with our finding that *ADTRP* is upstream of *MIA3/TANGO1*.

EAhy926 ECs transfected with an expression plasmid for *MIA3/TANGO1* and stimulated with ox-LDL showed significantly reduced adhesion to HL-60 cells compared with cells transfected with an empty vector ($P<0.0001$; Fig. 5H, 5G). Overexpression of *ADTRP* significantly reduced ox-LDL-induced adhesion of HL60 cells to EAhy926 ECs as compared with control vector, and the effect was further enhanced by overexpression of *MIA3/TAGO1* (Fig. 5H, 5F). *ADTRP* siRNA significantly increased ox-LDL-induced adhesion of HL60 cells to EAhy926 ECs as compared with NC siRNA, however, the effect was abolished by overexpression of *MIA3/TANGO1* (Fig. 5H, 5E), suggesting that *MIA3/TANGO* acts downstream of *ADTRP*.

For transmigration of HL-60 cells across the layer of EAhy926 cells stimulated with ox-LDL, *ADTRP* siRNA significantly increased the transmigration (Fig. 6A), whereas overexpression of *ADTRP* in EAhy926 cells inhibited the transmigration (Fig. 6B). Overexpression of *myrAKT* eliminated the increased transmigration by *ADTRP* siRNA, however, this effect was eliminated by PI3K inhibitor LY294002 (Fig. 6A). Overexpression of *ADTRP* and overexpression of *myrAKT* had an additive effect on inhibition of the transmigration, but the additive effect was eliminated by LY294002 (Fig. 6B).

MIA3/TANGO1 knockdown by siRNA in EAhy926 cells significantly increased the transmigration of HL-60 cells across the layer of EAhy926 cells stimulated with ox-LDL ($P=0.0003$, Fig. 6C). However, overexpression of *ADTRP* in EAhy926 cells did not have

any effect on the inhibitory effect of *MIA3/TANGO1* siRNA on the transmigration (Fig. 6C), which is consistent with our finding that *ADTRP* acts upstream of *MIA3/TANGO1*.

MIA3/TANGO1 overexpression by transient transfection with an expression plasmid for *MIA3/TANGO1* vs. an empty vector in EAhy926 cells significantly reduced transmigration of HL-60 cells across the layer of EAhy926 cells stimulated with ox-LDL ($P<0.0001$; Fig. 6E). Overexpression of *ADTRP* in EAhy926 cells significantly reduced transmigration of HL-60 cells across the layer of EAhy926 cells stimulated with ox-LDL as compared with vector control, which was further reduced by co-expression of both *MIA3/TANGO1* and *ADTRP* ($P=0.0047$; Fig. 6E). *ADTRP* siRNA significantly increased ox-LDL-induced transmigration of HL60 cells across EAhy926 ECs as compared with NC siRNA, however, the effect was abolished by overexpression of *MIA3/TANGO1* (Fig. 6D), suggesting that *MIA3/TANGO* acts downstream of *ADTRP*.

3.4. Effects of ADTRP and MIA3/TANGO1 knockdown or overexpression on other endothelial cell phenotypes

We previously showed that *ADTRP* regulated EC proliferation, apoptosis and migration [16]. As *ADTRP* exerts its effect through the AKT pathway, we studied the relationship between *ADTRP* and AKT in these cellular processes. *ADTRP* siRNA inhibited EAhy926 cell proliferation, however, overexpression of *myrAKT* increased EC proliferation and partially rescued the effect of *ADTRP* siRNA at 24 hr, 48 hr and 72 hr after transfection (Fig. 7A). Overexpression of either *ADTRP* or *myrAKT* increased EC proliferation, and overexpression of both genes further increased EC proliferation at all three tested time points (Fig. 7B). *ADTRP* siRNA inhibited EAhy926 cell proliferation, however, overexpression of *MIA3/TANGO1* partially rescued the effect of *ADTRP* siRNA at 24 hr, 48 hr and 72 hr after transfection (Fig. 7C). Overexpression of either *ADTRP* or *MIA3/TANGO1* significantly increased EC proliferation, and overexpression of both genes further increased EC proliferation at all three tested time points (Fig. 7D). Similar findings were made for the number of cells at the S phase during cell cycle progression (Fig. 8) and EC migration (Fig. 9 and Fig. S2, S3).

ADTRP siRNA significantly increased the rate of apoptosis of EAhy926 cells, but overexpression of either *myrAKT* or *MIA3/TANGO1* restored apoptosis to the basal level (Fig. 10A, 10B, 10E, 10F). Overexpression of either *ADTRP*, *myrAKT* or *MIA3/TANGO1* inhibited basal level apoptosis of EAhy926 cells, and overexpression of both *ADTRP* and *myrAKT* genes or both *ADTRP* and *MIA3/TANGO1* genes further reduced apoptosis (Fig. 10C, 10D, 10G, 10H). Similar results were obtained with HepG2 cells (Fig. S4, S5).

We further studied the capillary tube formation by EAhy926 cells. *ADTRP* siRNA inhibited capillary tube formation by EAhy926 cells, however, overexpression of *myrAKT* increased EC tube formation and rescued the effect of *ADTRP* siRNA (Fig. 11A–11D, 11K). The rescue effect of *myrAKT* on *ADTRP* siRNA was eliminated by PI3K inhibitor LY294002 (Fig. 11E, 11K). Overexpression of either *ADTRP* or *myrAKT* increased EC tube formation, and overexpression of both genes further increased EC tube formation (Fig. 11F–I, 11L). The stimulating effect of *ADTRP* and *myrAKT* on EC tube formation was eliminated by LY294002 (Fig. 11J, 11L). *ADTRP* siRNA inhibited capillary tube formation by EAhy926

cells, however, overexpression of *MIA3/TANGO1* partially rescued the effect of *ADTRP* siRNA (Fig. 11M–11P, 11U). Overexpression of either *ADTRP* or *MIA3/TANGO1* increased EC tube formation, and overexpression of both genes further increased EC tube formation (Fig. 11Q–11T, 11V).

3.5. Effects of ADTRP and MIA3/TANGO1 knockdown or overexpression on expression of collagen VII and ApoB

MIA3/TANG*O*1 is an endoplasmic reticulum transmembrane protein required for ER exit and secretion of large molecular such as collagen VII and ApoB [14]. To further validate the finding that *ADTRP* regulates expression of *MIA3/TANGO1*, we performed immunostaining analysis with an anti-collagen VII antibody or an anti-ApoB antibody in cells with knockdown or overexpression of *ADTRP*. Knockdown of *ADTRP* expression by siRNA significantly increased intracellular accumulation of collagen VII or ApoB in all three cell types analyzed (HepG2, HeLa, and HUVECs) (Fig. S6A–B, E–I and Fig. S7A–B, E–I). On the other hand, overexpression of *ADTRP* significantly decreased intracellular accumulation of collagen VII or ApoB (Fig. S6C–D, J and Fig. S7C–D, J).

We also used Western blot analysis to demonstrate that *ADTRP* negatively regulates the expression levels of collagen VII and ApoB in HepG2 and Eahy926 cells (Fig. 12). Knockdown of *ADTRP* expression by *ADTRP* siRNA significantly increased the expression level of collagen VII in HepG2 cells (Fig. 12A, 12B) and EAhy926 cells (Fig. 12C, 12D) as compared with NC siRNA. Knockdown of *ADTRP* expression by *ADTRP* siRNA significantly increased the expression level of ApoB in HepG2 cells (Fig. 12E, 12F) and EAhy926 cells (Fig. 12G, 12H) as compared with NC siRNA.

Altogether, our data uncovered a novel molecular signaling pathway that regulates the susceptibility to CAD and MI, mainly consisting of ADTRP, PIK3R3, AKT, MIA3/TANGO1 and collagen VII/ApoB (Fig. 13).

4. Discussion

In this study, we identified a molecular signaling pathway by which CAD susceptibility gene *ADTRP* functions in endothelial cellular processes relevant to atherosclerosis. *ADTRP* was previously referred to as *C6orf105*. In the First GWAS for CAD in the Chinese Han population, we found that a genomic variant in intron 1 of *ADTRP* (SNP rs6903956) showed significantly increased risk of CAD and MI [2]. Using global gene expression profiling and follow-up real-time RT-PCR and Western blot analyses, we have demonstrated that *ADTRP* positively regulates the expression of another CAD gene identified by GWAS, the *MIA3/TANGO1* gene (Fig. 1). Both *ADTRP* and *MIA3/TANGO1* are important susceptibility genes for CAD and MI in the Chinese population [2, 11]. We further demonstrated that *ADTRP* positively regulated the expression of *MIA3/TANGO1* by positively regulating expression of the *PIK3R3* gene, which leads to activation of AKT and upregulation of *MIA3/TANGO1* (Figs. 2–4). Both *ADTRP* and *MIA3/TANGO1* regulate monocyte adhesion to endothelial cells (Fig. 6) and transmigration of monocytes across endothelial cell layers (Fig. 5), two key processes required for the initiation of atherosclerosis. In sum, our

data identified a novel pathway involving *ADTRP-PIK3R3*-AKT activation-*MIA3/TANGO1* for the development of abnormal EC functions relevant to atherosclerosis and CAD.

Lupu et al reported that *ADTRP* expression was positively correlated with the expression level of TFPI (tissue factor pathway inhibitor) [7], which inhibits the activity of tissue factor FXa, coagulation and thrombosis. Reduced *ADTRP* expression by SNP rs6903956 may increase risk of MI by decreasing TFPI expression and increasing FXa activity and coagulation. Increased coagulation by reduced *ADTRP* expression may increase the risk of thrombosis and MI, but this hypothesis remains to be tested in the future. In this study, our data instead suggest that *ADTRP* may increase risk of CAD and MI by affecting the functions of ECs that are directly relevant to development of atherosclerosis. We found that reduced *ADTRP* expression increased ox-LDL-mediated monocyte adhesion to ECs, the first step involved in the initiation of atherosclerosis, and increased transendothelial migration of monocytes, another critical step in development of atherosclerosis (Fig. 5 and Fig. 6). Moreover, *ADTRP* positively regulates expression of *MIA3/TANGO1* (Fig. 1). Therefore, *ADTRP* may increase risk of CAD and MI by regulating the expression of the *MIA3/TANGO1* gene. MIA3/TANGO1 was initially found to be required for export of collagen VII from the ER [12]. Later, studies with *MIA3/TANGO1* knockout mice showed that it is required for secretion of not only collagen VII, but also collagens I, II, III, IV, and IX [13]. Fibrillar collagens are important components of atherosclerotic lesions. Excessive collagen accumulation may lead to stenosis of coronary arteries, whereas an inadequate amount of collagens may weaken plaques and cause plaque rupture, leading to MI. Fraccarollo et al showed association between decreased collagen gene expression and enhanced infarct expansion in a rat MI model [15]. Kong et al showed that the expression level of collagen III was decreased in aortic punch tissue samples from coronary artery bypass graft surgery from patients with acute MI [28].

Santos et al recently showed that MIA3/TANGO1 was required for the export of ApoB from the ER [14]. Because *ADTRP* regulates the expression level of *MIA3/TANGO1*, we examined the effect of *ADTRP* knockdown on the level of ApoB in cells. Interestingly, compared with NC siRNA, *ADTRP* siRNA significantly increased the level of ApoB in both HepG2 and Eahy926 cells (Fig. 12). ApoB is involved in transporting proatherogenic cholesterol particles (very low-density lipoprotein or VLDL, intermediate-density lipoprotein and LDL particles) [14]. The serum level of ApoB was considered to be a better predictive marker for the presence and severity of CAD and future outcomes than conventional lipid markers such as LDL-cholesterol levels [14]. Therefore, *ADTRP* variant may also increase risk of CAD and MI by regulating the cell level of ApoB.

In summary, here we have identified a novel biological pathway for the pathogenesis of CAD, which consists of *ADTRP-PIK3R3*-AKT activation-*MIA3/TANGO1*. The pathway is involved in monocyte adhesion to endothelial cells, transendothelial migration of monocytes, and other endothelial functions such as cell proliferation, migration, cell cycle regulation, apoptosis and endothelial tube formation.

Supplementary Material

Refer to Web version on PubMed Central for supplementary material.

Acknowledgments

We thank Dr. Vivek Malhotra, Dr. Ishier Raote and Dr. Maria Ortega Bellido for providing the mammalian expression plasmids for *MIA3/TANGO1*. We thank other members of Wang laboratory for help and assistance. We greatly appreciate all study subjects for their participation in this project.

Funding

This study was supported by the China National Natural Science Foundation Key Program (31430047 and 81630002), Chinese National Basic Research Programs (973 Programs 2013CB531101 and 2012CB517801), Hubei Province's Outstanding Medical Academic Leader Program, Hubei Province Natural Science Key Program (2014CFA074), the China National Natural Science Foundation grants (91439129， NSFC-J1103514, 81370206), NIH/NHLBI grants R01 HL121358 and R01 HL126729, a Key Project in the National Science & Technology Pillar Program during 395 the Twelfth Five-year Plan Period (2011BAI11B19), Specialized Research Fund for the Doctoral Program of Higher Education from the Ministry of Education, and the "Innovative Development of New Drugs" Key Scientific Project (2011ZX09307-001-09).

References

1. Libby P. Inflammation in atherosclerosis. Nature. 2002; 420:868–874. [PubMed: 12490960]
2. Wang F, Xu CQ, He Q, Cai JP, Li XC, Wang D, Xiong X, Liao YH, Zeng QT, Yang YZ, Cheng X, Li C, Yang R, Wang CC, Wu G, Lu QL, Bai Y, Huang YF, Yin D, Yang Q, Wang XJ, Dai DP, Zhang RF, Wan J, Ren JH, Li SS, Zhao YY, Fu FF, Huang Y, Li QX, Shi SW, Lin N, Pan ZW, Li Y, Yu B, Wu YX, Ke YH, Lei J, Wang N, Luo CY, Ji LY, Gao LJ, Li L, Liu H, Huang EW, Cui J, Jia N, Ren X, Li H, Ke T, Zhang XQ, Liu JY, Liu MG, Xia H, Yang B, Shi LS, Xia YL, Tu X, Wang QK. Genome-wide association identifies a susceptibility locus for coronary artery disease in the Chinese Han population. Nat Genet. 2011; 43:345–349. [PubMed: 21378986]
3. Guo CY, Gu Y, Li L, Jia EZ, Li CJ, Wang LS, Yang ZJ, Cao KJ, Ma WZ. Association of SNP Rs6903956 on Chromosome 6p24.1 with Angiographical Characteristics of Coronary Atherosclerosis in a Chinese Population. PLoS One. 2012; 7:e43732. [PubMed: 22952750]
4. Tayebi N, Ke T, Foo JN, Friedlander Y, Liu J, Heng CK. Association of single nucleotide polymorphism rs6903956 on chromosome 6p24.1 with coronary artery disease and lipid levels in different ethnic groups of the Singaporean population. Clin Biochem. 2013; 46:755–759. [PubMed: 23337689]
5. Huang EW, Peng LY, Zheng JX, Wang D, Xu QY, Huang L, Wu QP, Tang SB, Luo B, Liu SP, Liu XS, Li ZH, Quan L, Li Y, Shi H, Lv GL, Zhao J, Cheng JD, Liu C. Common Variants in Promoter of ADTRP Associate with Early-Onset Coronary Artery Disease in a Southern Han Chinese Population. PLoS One. 2015; 10:e0137547. [PubMed: 26375920]
6. Liu X, Zhang M, Shan HW, Song XT, Lyu SZ. Association of single nucleotide polymorphism rs2076185 in chromosome 6P24.1 with premature coronary artery diseases in Chinese Han population. J Geriatr Cardiol. 2016; 13:138–144. [PubMed: 27168739]
7. Lupu C, Zhu H, Popescu NI, Wren JD, Lupu F. Novel protein ADTRP regulates TFPI expression and function in human endothelial cells in normal conditions and in response to androgen. Blood. 2011; 118:4463–4471. [PubMed: 21868574]
8. Chinetti-Gbaguidi G, Copin C, Derudas B, Vanhoutte J, Zawadzki C, Jude B, Haulon S, Pattou F, Marx N, Staels B. The coronary artery disease-associated gene C6ORF105 is expressed in human macrophages under the transcriptional control of PPARgamma. FEBS Lett. 2015; 589:461–466. [PubMed: 25595457]
9. Roberts R. A genetic basis for coronary artery disease. Trends Cardiovas Med. 2015; 25:171–178.
10. Wang AZ, Li L, Zhang B, Shen GQ, Wang QK. Association of SNP rs17465637 on chromosome 1q41 and rs599839 on 1p13.3 with myocardial infarction in an American caucasian population. Ann Hum Gene. 2011; 75:475–482.

11. Li X, Huang Y, Yin D, Wang D, Xu C, Wang F, Yang Q, Wang X, Li S, Chen S, Xiong X, Huang Y, Zhao Y, Wang L, Zhu X, Su Z, Zhou B, Zhang Y, Wang L, Chang L, Xu C, Li H, Ke T, Ren X, Cheng X, Yang Y, Liao Y, Tu X, Wang QK. Meta-analysis identifies robust association between SNP rs17465637 in MIA3 on chromosome 1q41 and coronary artery disease. Atherosclerosis. 2013; 231:136–140. [PubMed: 24125424]
12. Saito K, Chen M, Bard F, Chen S, Zhou H, Woodley D, Polischuk R, Schekman R, Malhotra V. TANGO1 facilitates cargo loading at endoplasmic reticulum exit sites. Cell. 2009; 136:891–902. [PubMed: 19269366]
13. Wilson DG, Phamluong K, Li L, Sun M, Cao TC, Liu PS, Modrusan Z, Sandoval WN, Rangell L, Carano RA, Peterson AS, Solloway MJ. Global defects in collagen secretion in a Mia3/TANGO1 knockout mouse. J Cell Biol. 2011; 193:935–951. [PubMed: 21606205]
14. Santos AJM, Nogueira C, Ortega-Bellido M, Malhotra V. TANGO1 and Mia2/cTAGE5 (TALI) cooperate to export bulky pre-chylomicrons/VLDLs from the endoplasmic reticulum. J Cell Biol. 2016; 213:343–354. [PubMed: 27138255]
15. Fraccarollo D, Galuppo P, Bauersachs J, Ertl G. Collagen accumulation after myocardial infarction: effects of ETA receptor blockade and implications for early remodeling. Cardiovasc Res. 2002; 54:559–567. [PubMed: 12031701]
16. Luo C, Wang F, Qin S, Chen Q, Wang QK. Coronary artery disease susceptibility gene ADTRP regulates cell cycle progression, proliferation, and apoptosis by global gene expression regulation. Physiol Genomics. 2016; 48:554–564. [PubMed: 27235449]
17. Malhotra V, Erlmann P, Nogueira C. Procollagen export from the endoplasmic reticulum. Biochem Soc T. 2015; 43:104–107.
18. Malhotra V, Erlmann P. The pathway of collagen secretion. Annu Rev Cell Dev Bi. 2015; 31:109–124.
19. Nogueira C, Erlmann P, Villeneuve J, Santos AJ, Martinez-Alonso E, Martinez- Menarguez JA, Malhotra V. SLY1 and Syntaxin 18 specify a distinct pathway for procollagen VII export from the endoplasmic reticulum. E Life. 2014; 3:e02784. [PubMed: 24842878]
20. Santos AJ, Raote I, Scarpa M, Brouwers N, Malhotra V. TANGO1 recruits ERGIC membranes to the endoplasmic reticulum for procollagen export. E Life. 2015; 4:e10982. [PubMed: 26568311]
21. Huang Y, Wang Z, Liu Y, Xiong H, Zhao Y, Wu L, Yuan C, Wang L, Hou Y, Yu G, Huang Z, Xu C, Chen Q, Wang QK. alphaB-Crystallin Interacts with Nav1.5 and Regulates Ubiquitination and Internalization of Cell Surface Nav1.5. J Biol Chem. 2016; 291:11030–11041. [PubMed: 26961874]
22. Xu Y, Zhou M, Wang J, Zhao Y, Li S, Zhou B, Su Z, Xu C, Xia Y, Qian H, Tu X, Xiao W, Chen X, Chen Q, Wang QK. Role of microRNA-27a in down-regulation of angiogenic factor AGGF1 under hypoxia associated with high-grade bladder urothelial carcinoma. BBA-Mol Basis Dis. 2014; 1842:712–725.
23. You SA, Archacki SR, Angheloiu G, Moravec CS, Rao S, Kinter M, Topol EJ, Wang Q. Proteomic approach to coronary atherosclerosis shows ferritin light chain as a significant marker: evidence consistent with iron hypothesis in atherosclerosis. Physiol Genomics. 2003; 13:25–30. [PubMed: 12644631]
24. Zhou B, Si W, Su Z, Deng W, Tu X, Wang Q. Transcriptional activation of the Prox1 gene by HIF-1α and HIF-2α in response to hypoxia. FEBS Lett. 2013; 587:724–731. [PubMed: 23395615]
25. Fan C, Ouyang P, Timur AA, He P, You SA, Hu Y, Ke T, Driscoll DJ, Chen Q, Wang QK. Novel Roles of GATA1 in Regulation of Angiogenic Factor AGGF1 and Endothelial Cell Function. J Biol Chem. 2009; 284:23331–23343. [PubMed: 19556247]
26. Zhou B, Ma R, Si W, Li S, Xu Y, Tu X, Wang Q. MicroRNA-503 targets FGF2 and VEGFA and inhibits tumor angiogenesis and growth. Cancer Lett. 2013; 333:159–169. [PubMed: 23352645]
27. Archacki SR, Angheloiu G, Moravec CS, Liu H, Topol EJ, Wang QK. Comparative gene expression analysis between coronary arteries and internal mammary arteries identifies a role for the TES gene in endothelial cell functions relevant to coronary artery disease. Hum Mol Genet. 2012; 21:1364–1373. [PubMed: 22156939]

28. Kong CH, Lin XY, Woo CC, Wong HC, Lee CN, Richards AM, Sorokin VA. Characteristics of aortic wall extracellular matrix in patients with acute myocardial infarction: tissue microarray detection of collagen I, collagen III and elastin levels. Interact Cardiov Th. 2013; 16:11–15.

Highlights

1. CAD susceptibility gene *ADTRP* positively regulates the expression level of another CAD susceptibility gene *MIA3/TANGO1.*
2. Both *ADTRP* and *MIA3/TANGO1* regulate endothelial cell phenotypes relevant to atherosclerosis, but *ADTRP* acts upstream of *MIA3/TANGO1.*
3. *ADTRP* positively regulates *MIA3/TANGO1* expression by positive regulation of *PIK3R3*, followed by activation of AKT.
4. *ADTRP* regulates the levels of large proteins such as collagen VII and ApoB in HepG2 and EAhy926 endothelial cells, the downstream targets of MIA3/TANGO1.

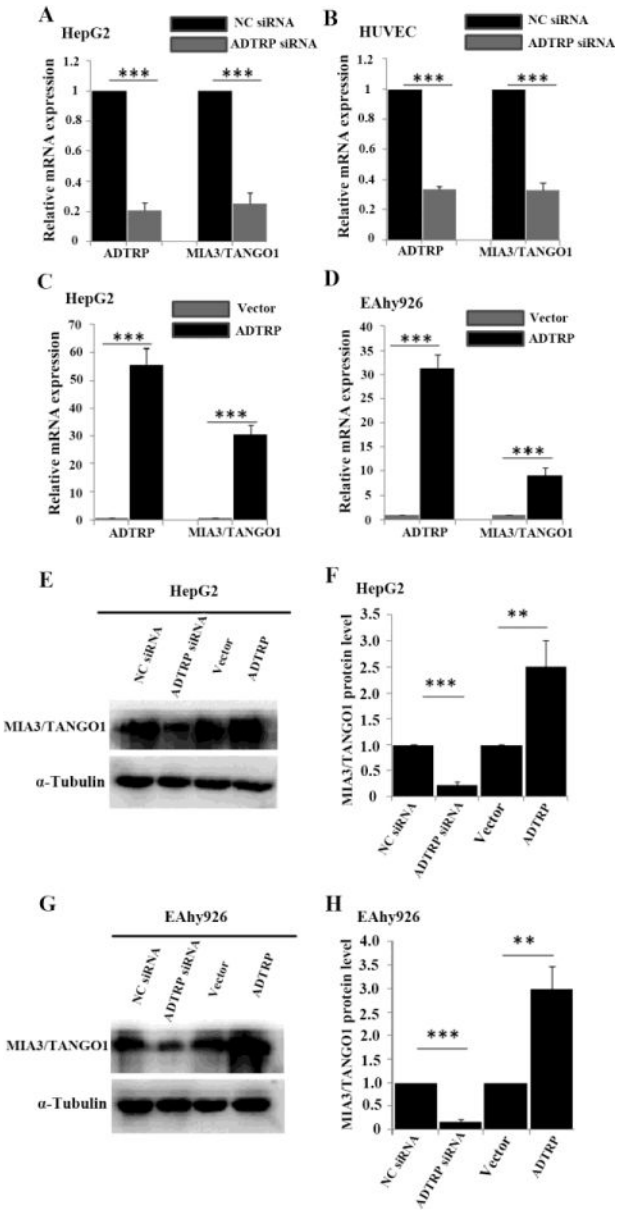

Fig. 1.

MIA3/TANGO1 is a downstream target gene regulated by *ADTRP*. (A) Real-time RT-PCR analysis for the expression levels of *ADTRP* and *MIA3/TANGO1* in HepG2 cells transfected with *ADTRP* siRNA or negative control (NC) siRNA. (B) Similar analysis as in (A) but in HUVECs. (C) Real-time RT-PCR analysis for expression of *ADTRP* and *MIA3/TANGO1* in HepG2 cells transfected with an expression plasmid for *ADTRP* or empty vector control. (D) Similar analysis as in (C) but in EAhy926 endothelial cells. (E) Western blot analysis for expression of MIA3/TANGO1 with knockdown of *ADTRP* expression with *ADTRP* siRNA (NC siRNA as control) or overexpression of *ADTRP* in HepG2 cells. α-tubulin was used as loading control. (F) Summary data from Western blot analysis as shown in (E). (G) Similar analysis as in (E) but in EAhy926 endothelial cells. (H) Summary data

from Western blot analysis as shown in (G). Each experiment was repeated at least three times. **, $P<0.01$; ***, $P<0.001$.

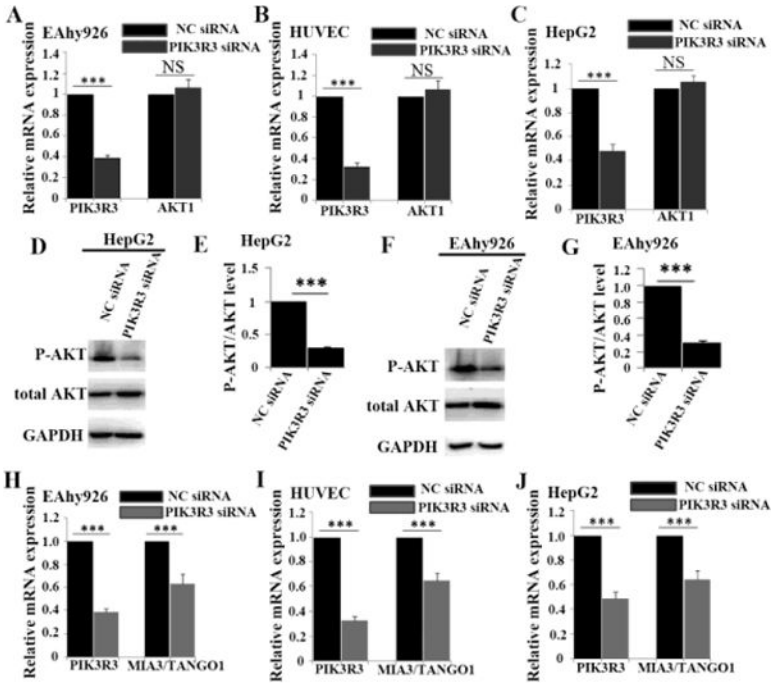

Fig. 2.

ADTRP downstream gene *PIK3R3* regulates AKT phosphorylation and *MIA3/TANGO1* expression. (A) Real-time RT-PCR analysis for the expression levels of *PIK3R3* and *AKT1* in EAhy926 cells transfected with *PIK3R3* siRNA (NC siRNA as control). (B) Similar analysis as in (A) but in HUVECs. (C) Similar analysis as in (A) but in HepG2 cells. (D) Western blot analysis for the expression levels of total AKT protein and phosphorylated AKT (P-AKT) after *PIK3R3* was knocked down by siRNA in HepG2 cells. GAPDH was used as loading control. (E) The ratio of P-AKT over total-AKT from Western blot images as in (D) was plotted. (F) Similar analysis as in (D) but in EAhy926 endothelial cells. (G) Summary data from Western blot analysis as shown in (F). (H) Real-time RT-PCR analysis for the expression levels of *PIK3R3* and *MIA3/TANGO1* in EAhy926 cells transfected with *PIK3R3* siRNA (NC siRNA as control). (I) Similar analysis as in (H) but in HUVECs. (J) Similar analysis as in (H) but in HepG2 cells. Each experiment was repeated at least three times. ***, $P<0.001$; NS, not significant.

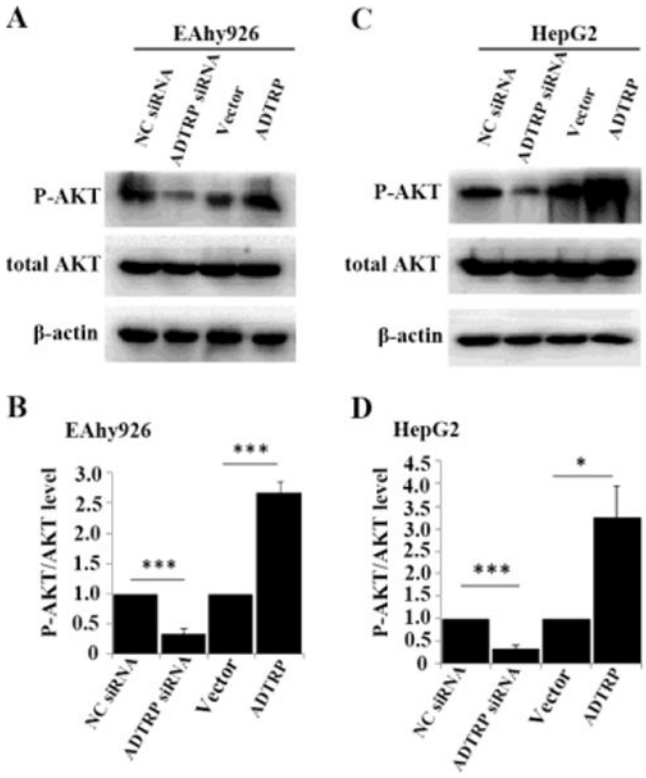

Fig. 3.

ADTRP regulates the phosphorylation level of AKT. (A) Western blot analysis for the expression levels of total AKT and phosphorylated AKT (P-AKT) after *ADTRP* was knocked down by siRNA (vs. NC siRNA) or overexpressed (ADTRP vs. vector) in EAhy926 cells. β-actin was used as loading control. (B) The ratio of P-AKT over total AKT from Western blot images as in (A) was plotted. (C) Similar analysis as in (A) but in HepG2 cells. (D) Summary data from Western blot analysis as shown in (C). Each experiment was repeated at least three times. ***, $P<0.001$.

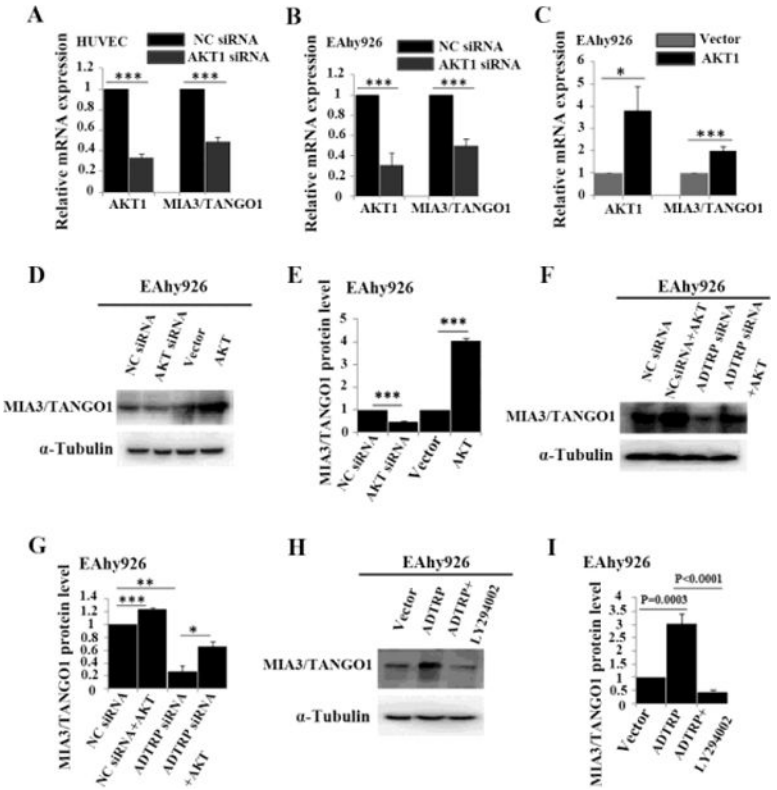

Fig. 4.

ADTRP regulates *MIA3/TANGO1* expression through the AKT signaling pathway. (A) Real-time RT-PCR analysis showing that knockdown of *AKT1* expression by siRNA (NC siRNA as control) reduced *MIA3/TANGO1* expression in HUVEC cells. (B) Real-time RT-PCR analysis showing that knockdown of *AKT1* expression by siRNA (NC siRNA as control) reduced *MIA3/TANGO1* expression in EAhy926 cells. (C) Real-time RT-PCR analysis showing that overexpression of *myrAKT1* by transfection of a myrAKT1 expression plasmid (vector as control) increased *MIA3/TANGO1* expression in EAhy926 cells. (D) Western blot analysis showing that knockdown of *AKT1* expression by siRNA reduced MIA3/TANGO1 expression and overexpression of *myrAKT1* increased MIA3/TANGO1 expression in EAhy926 cells. (E) Summary data from Western blot analysis as shown in (D). (F) Western blot analysis showing that reduced MIA3/TANGO1 expression by *ADTRP* siRNA was partially rescued by co-expression of *myrAKT1*. (G) Summary data from Western blot analysis as shown in (F). (H) Western blot analysis showing that increased expression of MIA3/TANGO1 by *ADTRP* overexpression was blocked by PI3K inhibitor LY294002 (20μM) in EAhy926 cell. (I) Summary data from Western blot analysis as shown in (H). Each experiment was repeated at least three times. *, $P<0.05$; **, $P<0.01$; ***, $P<0.001$.

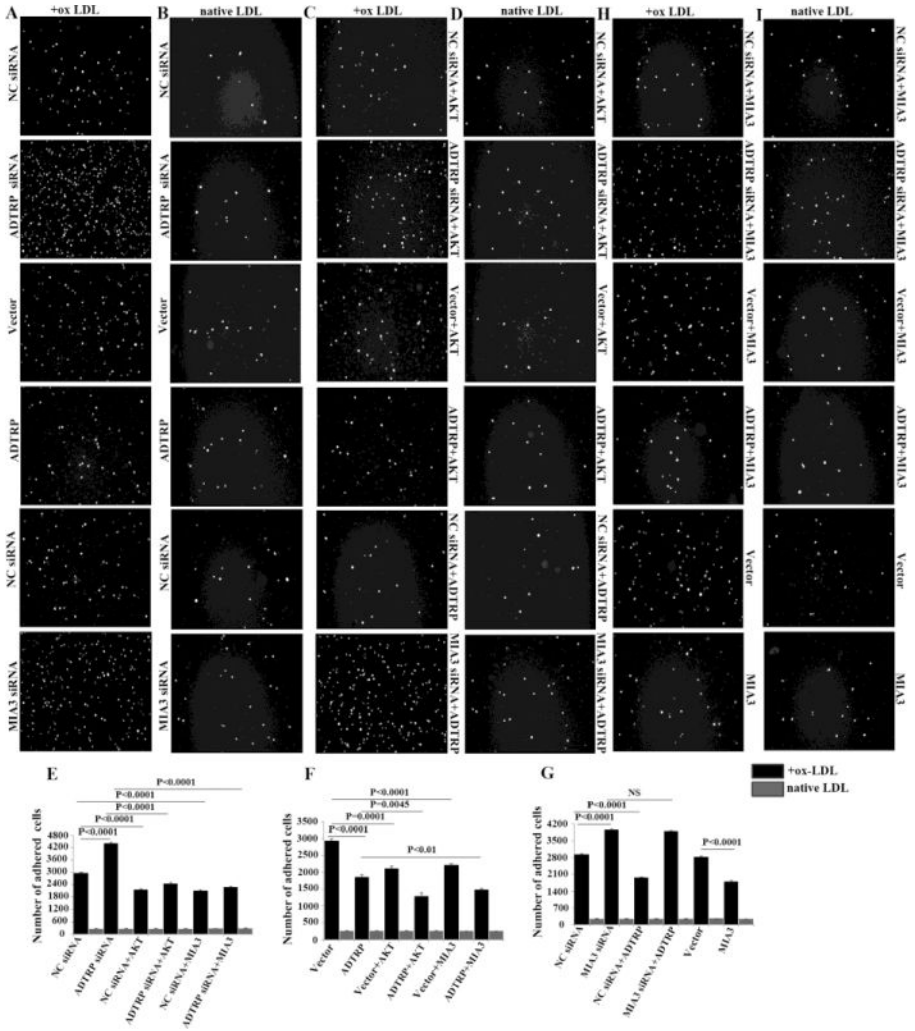

Fig. 5.

ADTRP regulates ox-LDL-mediated monocyte adhesion to endothelial cells (ECs) by mediating activation of AKT. (A) Representative images for analysis of monocyte adhesion to ECs (EAhy926 cells) stimulated by ox-LDL for *ADTRP* siRNA vs. NC siRNA, *ADTRP* expression plasmid vs. vector, *MIA3* siRNA vs. NC siRNA. (B) Similar analyses as in (A) but with EAhy926 cells without ox-LDL stimulation. (C) Similar analyses as in (A) for *ADTRP* siRNA in the presence of hmyrAKT1 vs. NC siRNA in the presence of hmyrAKT1, ADTRP in the presence of hmyrAKT1 vs. vector in the presence of hmyrAKT1, *MIA3* siRNA in the presence of *ADTRP* vs. NC siRNA in the presence of *ADTRP*. (D) Similar analyses as in (C) but with EAhy926 cells without ox-LDL stimulation. (E, F, G) Summary data from experiments as shown in (A–I). Each experiment was repeated at least three times. (H) Similar analyses as in (A) for *ADTRP* siRNA vs. NC siRNA with overexpression of *MIA3/TANGO1*, *ADTRP* expression plasmid vs. vector control with overexpression of *MIA3/TANGO1*, and *MIA3/TANGO1* expression plasmid vs. vector in EAhy926 cells with ox-LDL stimulation. (I) Similar analyses as in (H) but in EAhy926 cells without ox-LDL stimulation. NS, not significant.

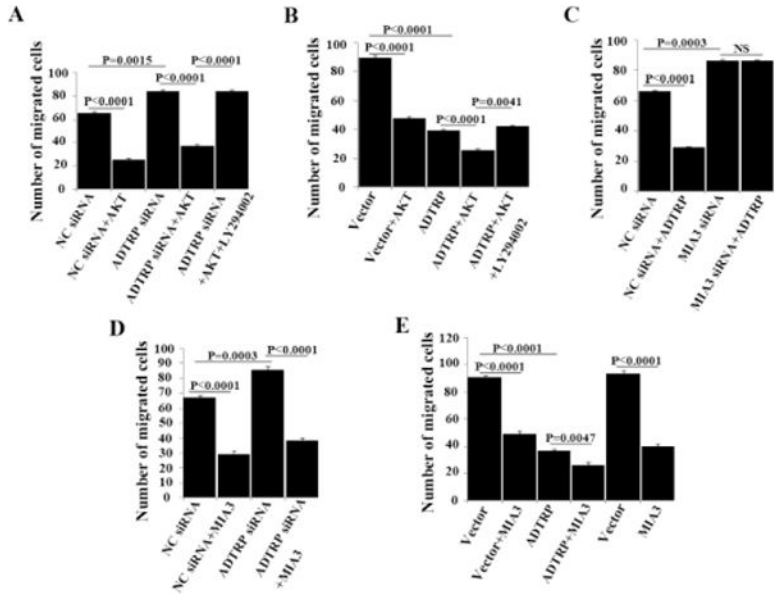

Fig. 6.

ADTRP regulates ox-LDL-mediated transmigration of monocytes across a layer of ECs by mediating activation of AKT. (A) Analysis of transmigration of monocytes across ox-LDL-treated EAhy926 cells for *ADTRP* siRNA vs. NC siRNA, *ADTRP* siRNA in the presence of hmyrAKT1 vs. NC siRNA in the presence of hmyrAKT1, *ADTRP* siRNA in the presence of hmyrAKT1 and LY294002. (B) Analysis of transmigration of monocytes across ox-LDL-treated EAhy926 cells for ADTRP vs. vector, ADTRP in the presence of hmyrAKT1 vs. vector in the presence of hmyrAKT1, ADTRP in the presence of hmyrAKT1and LY294002. (C) Analysis of transmigration of monocytes across ox-LDL-treated EAhy926 cells for *MIA3/TANGO1* siRNA vs. NC siRNA, *MIA3/TANGO1* siRNA in the presence of ADTRP vs. NC siRNA in the presence of ADTRP. Each experiment was repeated at least three times. (D) Analysis of transmigration of HL60 monocytes across ox-LDL-treated EAhy926 cells transfected with *ADTRP* siRNA vs. NC siRNA, and *ADTRP* siRNA in the presence of *MIA3/TANGO1* vs. NC siRNA in the presence of *MIA3/TANGO1*. (E) Analysis of transmigration of HL60 monocytes across ox-LDL-treated EAhy926 cells transfected with *ADTRP* expression plasmid vs. vector control, *ADTRP* overexpression in the presence of *MIA3/TANGO1* expression plasmid vs. vector control, and *MIA3/TANGO1* expression plasmid vs. vector control. NS, not significant.

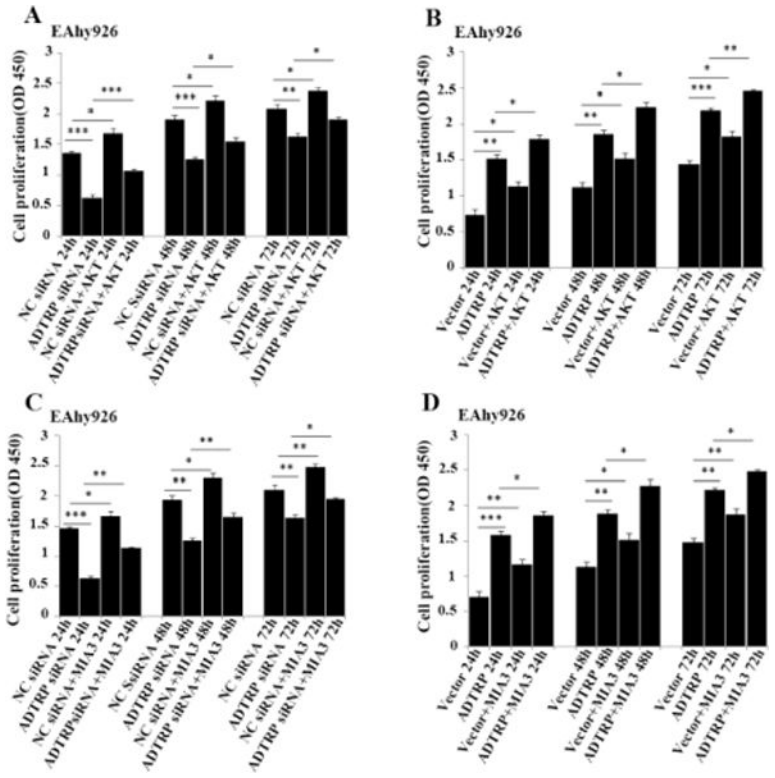

Fig. 7.

Effect of AKT on *ADTRP-MIA3/TANGO1* regulation on cell proliferation. EAhy926 cells were transfected with different siRNA or expression plasmids, cultured for 24 hr, 48 hr and 72 hr, and used for measuring the number of living cells using the CCK8 kit. (A) Cell proliferation analysis for knockdown of *ADTRP* in the presence or absence of *myrAKT*. (B) Cell proliferation analysis for overexpression of *ADTRP* in the presence or absence of *myrAKT*. Each experiment was repeated at least three times. (C) Cell proliferation analysis for knockdown of *ADTRP* in the presence or absence of *MIA3/TANGO1* overexpression. (D) Cell proliferation analysis for overexpression of *ADTRP* in the presence or absence of *MIA3/TANGO1* overexpression. *, $P<0.05$; **, $P<0.01$; ***, $P<0.001$.

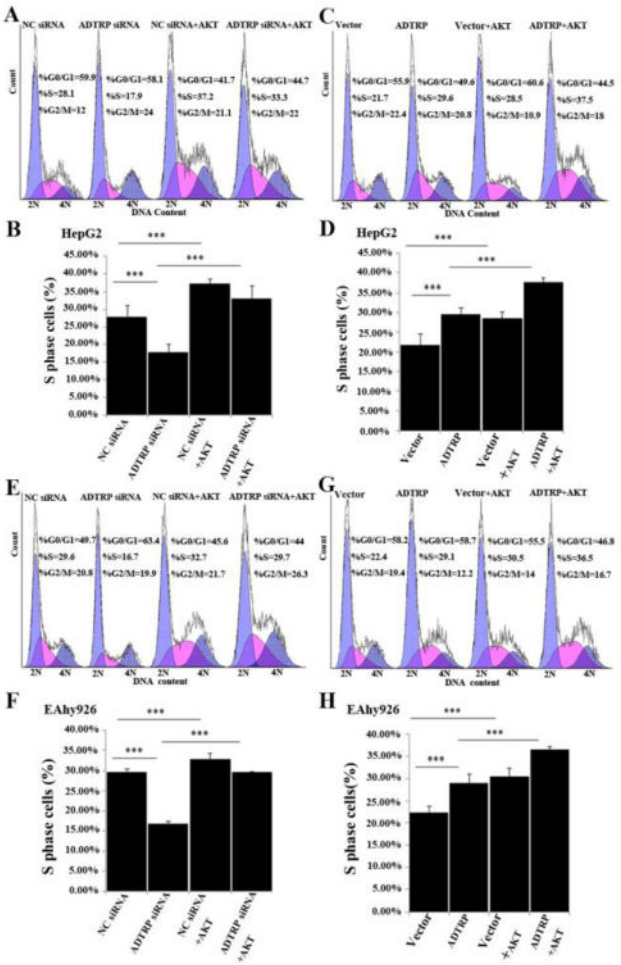

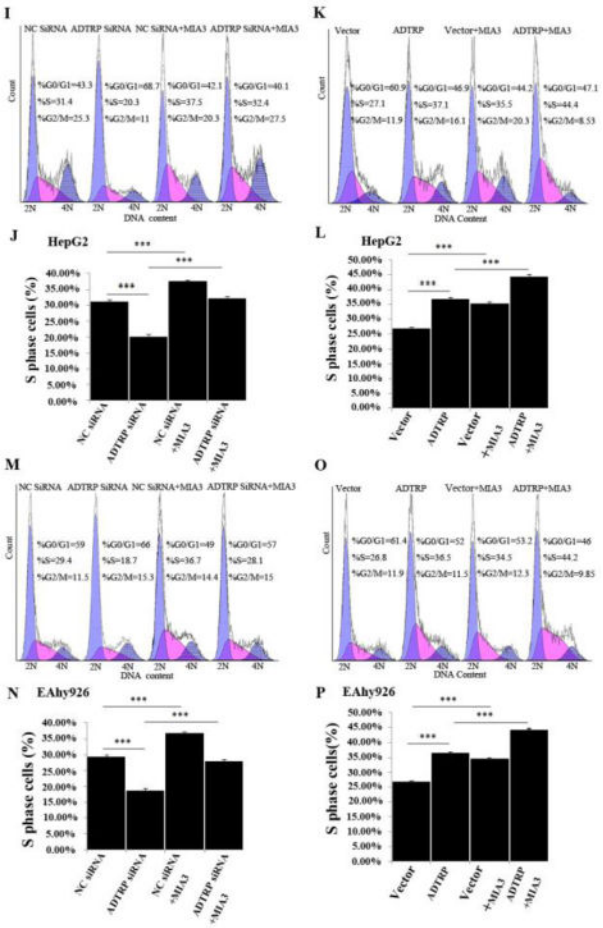

Fig. 8.

Effect of *AKT* or *MIA3/TANGO1* on *ADTRP* regulation of cell cycle progression. (A) Representative flow cytometry data showing the cell number at the S phase of cell cycle for knockdown of *ADTRP* in the presence or absence of *myrAKT* in HepG2 cells. (B) Summary data from experiments as shown in (A). (C) Representative flow cytometry data showing the cell number at the S phase of cell cycle for overexpression of *ADTRP* in the presence or absence of *myrAKT* in HepG2 cells. (D) Summary data from experiments as shown in (C). (E, F, G, H) Similar to A, B, C, and D, respectively, but in EAhy926 cells. (I) Representative flow cytometry data showing the cell number at the S phase of cell cycle for knockdown of *ADTRP* in the presence or absence of *MIA3/TANGO1* overexpression in HepG2 cells. (J) Summary data from experiments as shown in (I). (K) Representative flow cytometry data showing the cell number at the S phase of cell cycle for overexpression of *ADTRP* in the presence or absence of *MIA3/TANGO1* overexpression in HepG2 cells. (L) Summary data from experiments as shown in (K). (M, N, O, P) Similar to I, J, K, and L, respectively, but in EAhy926 cells. Each experiment was repeated at least three times. ***, $P<0.001$.

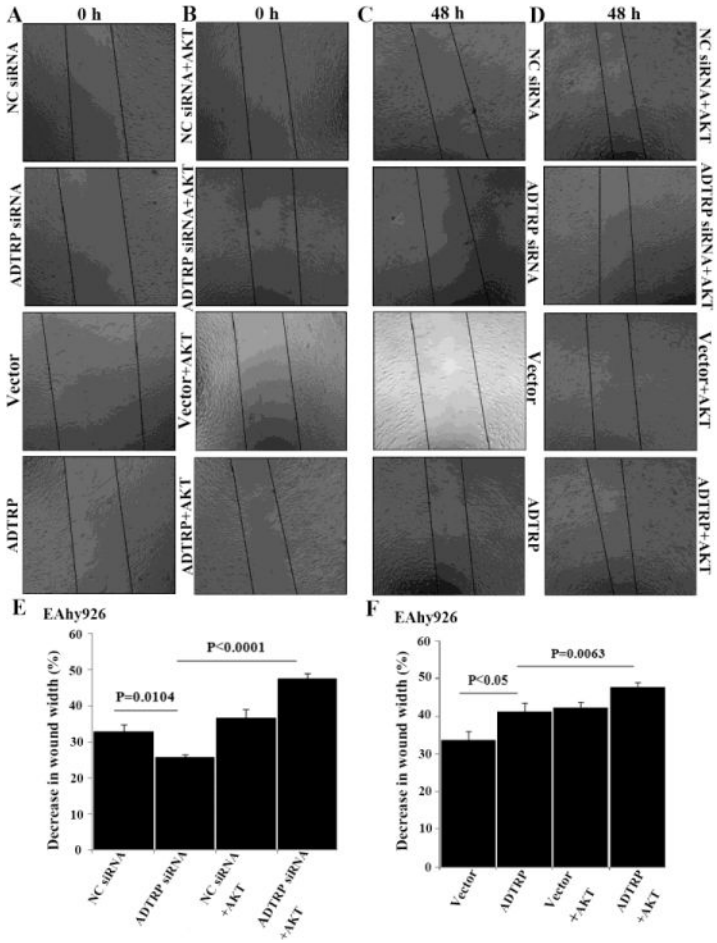

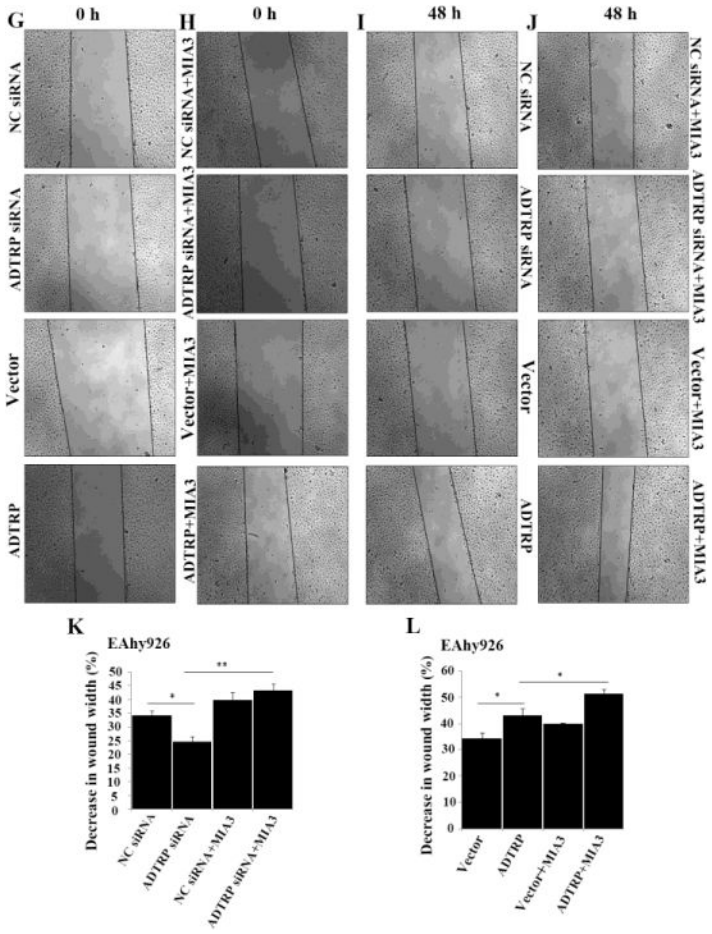

Fig. 9.

Effect of *AKT* or *MIA3/TANGO1* on *ADTRP* regulation of cell migration. (A, B, C, D) Representative images for scratch-based cell migration analysis for EAhy926 cells with different treatments for *ADTRP* and *myrAKT*. (E) Summary data from (A–D) for cell migration analysis for knockdown of *ADTRP* in the presence or absence of *myrAKT*. (F) Summary data from (A–D) for cell migration analysis for overexpression of *ADTRP* in the presence or absence of *myrAKT*. (G–J) Representative images for scratch-based cell migration analysis for EAhy926 cells with different treatments for *ADTRP* and *MIA3/TANGO1*. (K) Summary data from (G–J) for cell migration analysis for knockdown of *ADTRP* in the presence or absence of *MIA3/TANGO1* overexpression. (L) Summary data from (G–J) for cell migration analysis for overexpression of *ADTRP* in the presence or absence of MIA3/TANGO1 overexpression. Each experiment was repeated at least three times. *, $P<0.05$; **, $P<0.01$.

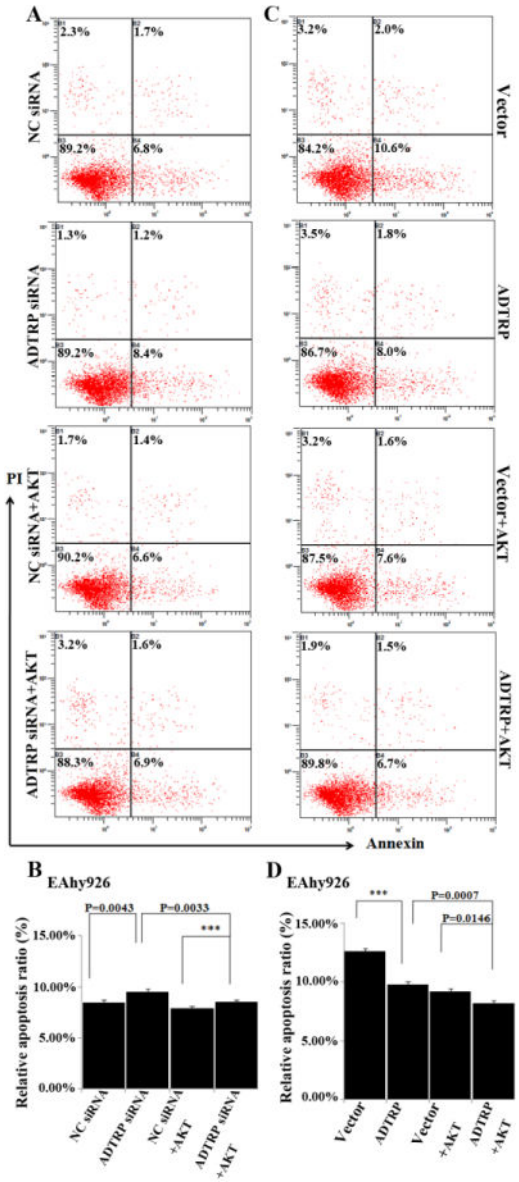

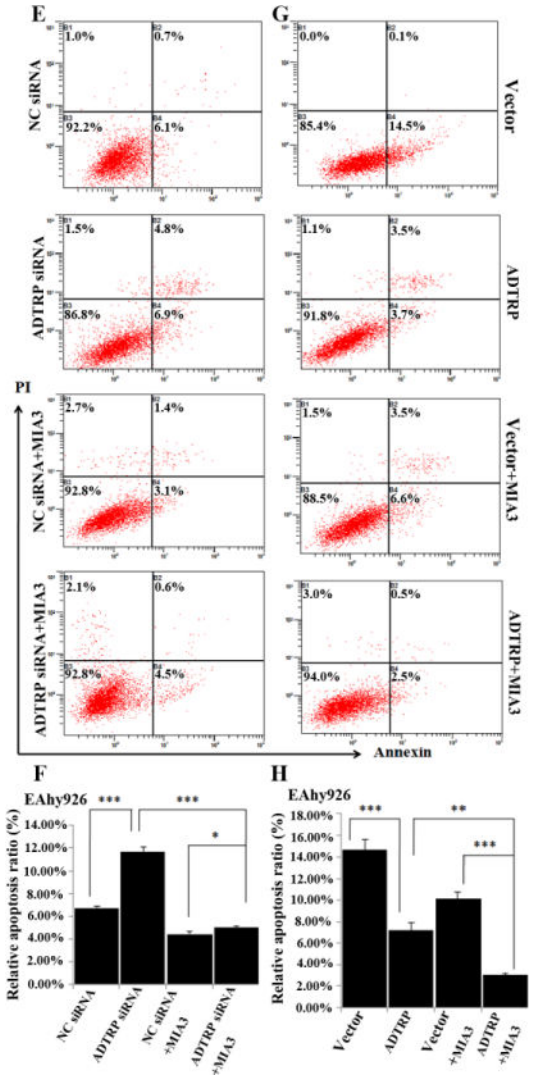

Fig. 10.

(1) Effect of *AKT* and *MIA3/TANGO1* on *ADTRP* regulation of apoptosis. (A) Representative flow cytometry images for analysis of apoptosis for *ADTRP* siRNA vs. NC siRNA, and *ADTRP* siRNA in the presence of hmyrAKT1vs. NC siRNA in the presence of hmyrAKT1 in EAhy926 cells. (B) Summary data from experiments as shown in (A). (C) Representative flow cytometry images for analysis of apoptosis for EAhy926 cells transfected with pcDNA3.1(−)-ADTRP vs. cells transfected with empty vector pcDNA3.1(−), and pcDNA3.1(−)-ADTRP together with pcDNA3.1(−)-myrAKT1 vs. pcDNA3.1(−) together with pcDNA3.1(−)-myrAKT1. (D) Summary data from experiments as shown in (C). (E) Representative flow cytometry images for analysis of apoptosis for *ADTRP* siRNA vs. NC siRNA, and *ADTRP* siRNA in the presence of *MIA3/TANGO1* overexpression vs. NC siRNA in the presence of *MIA3/TANGO1* overexpression in EAhy926 cells. (F) Summary data from experiments as shown in (A). (G) Representative flow cytometry images for analysis of apoptosis for EAhy926 cells transfected with pcDNA3.1(−)-ADTRP vs. cells transfected with empty vector pcDNA3.1(−), and pcDNA3.1(−)-ADTRP together with pcDNA3.1(+)-MIA3/TANGO1 vs. pcDNA3.1(+)

together with pcDNA3.1(+)-MIA3/TANGO1. (H) Summary data from experiments as shown in (C). Each experiment was repeated at least three times. *, $P<0.05$; **, $P<0.01$; ***, $P<0.001$.

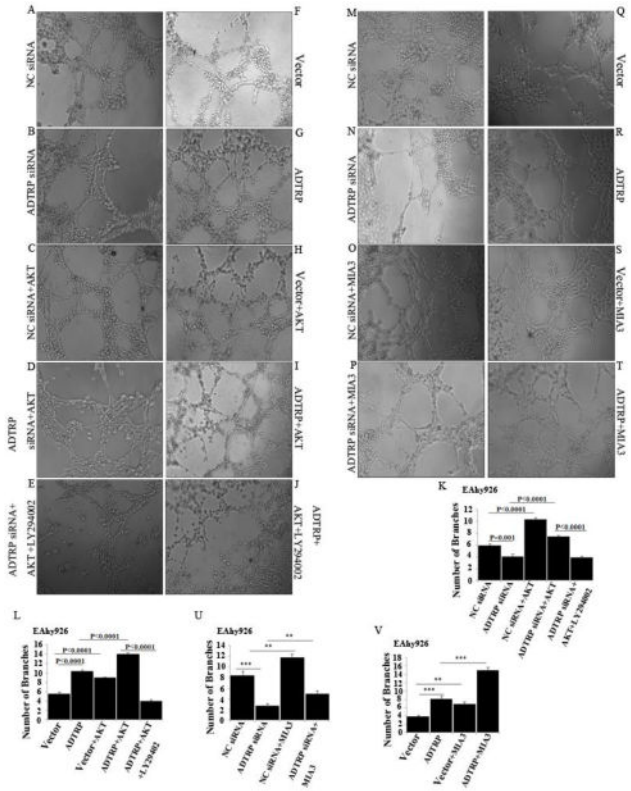

Fig. 11.

ADTRP regulates EC capillary tube formation through the AKT signaling pathway and *MIA3/TANGO1*. (A–J) Representative images for capillary tube formation by EAhy926 cells with different treatments for *ADTRP* and *AKT*. (K) Summary data from experiments as shown in (A–E) for capillary tube formation in EAhy926 cells with knockdown of *ADTRP* and effects of *myrAKT* and LY294002. (L) Summary data from experiments as shown in (F–J) for capillary tube formation in EAhy926 cells with overexpression of *ADTRP* and effects of *myrAKT* and LY294002. (M–T) Representative images for capillary tube formation by EAhy926 cells with different treatments for *ADTRP* and *MIA3/TANGO1*. (U) Summary data from experiments as shown in (M–P) for capillary tube formation in EAhy926 cells with knockdown of *ADTRP* with or without overexpression of *MIA3/TANGO1*. (V) Summary data from experiments as shown in (Q–T) for capillary tube formation in EAhy926 cells with overexpression of *ADTRP*, *MIA3/TANGO1*, or both. Each experiment was repeated at least three times. **, $P<0.01$; ***, $P<0.001$.

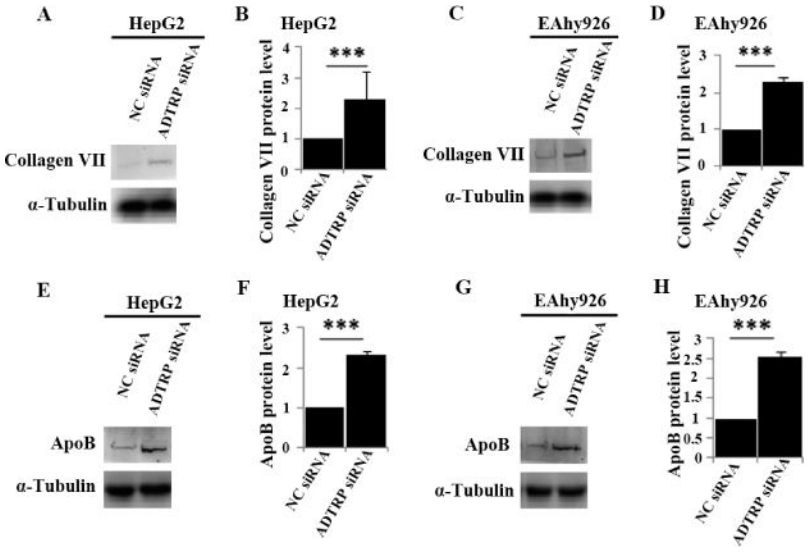

Fig. 12.

ADTRP regulates *Collagen VII* and *ApoB* expression. (A) Western blot analysis showing increased *Collagen VII* expression after *ADTRP* knockdown by siRNA in HepG2 cell. (B) Summary data from Western blot analysis as shown in (A). (C) Western blot analysis showing increased *Collagen VII* expression after *ADTRP* knockdown by siRNA in EAhy926 cell. (D) Summary data from Western blot analysis as shown in (C). (E) Western blot analysis showing increased *ApoB* expression after *ADTRP* knockdown by siRNA in HepG2 cell. (F) Summary data from Western blot analysis as shown in (E). (G) Western blot analysis showing increased *ApoB* expression after *ADTRP* knockdown by siRNA in EAhy926 cell. (H) Summary data from Western blot analysis as shown in (E).

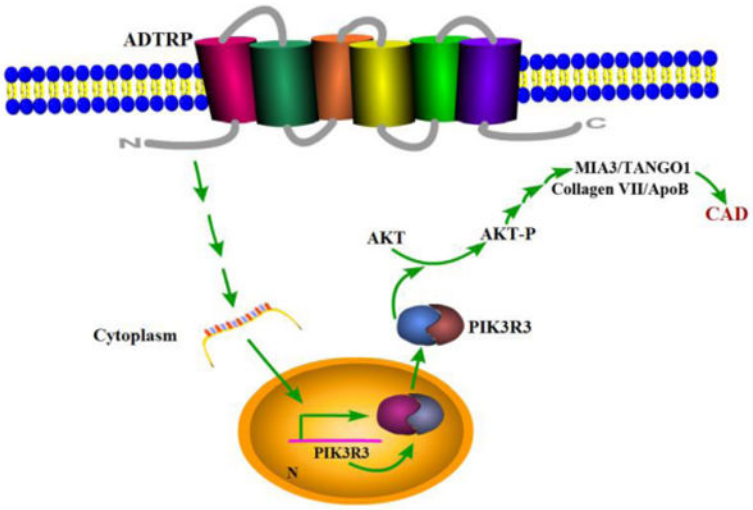

Fig. 13.
Schematic diagram for the ADTRP signaling pathway.